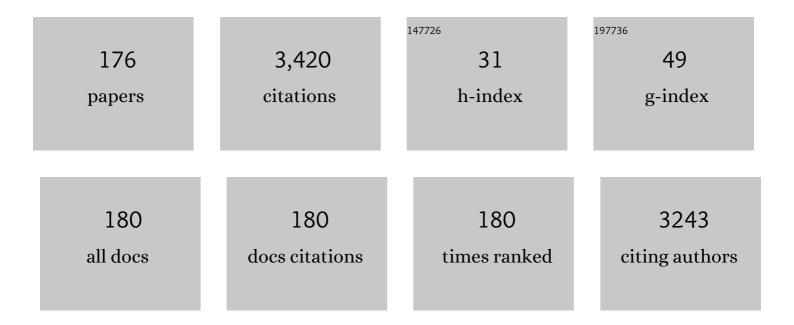
List of Publications by Year in descending order

Source: https://exaly.com/author-pdf/191588/publications.pdf Version: 2024-02-01



S W KINC

#	Article	IF	CITATIONS
1	Cleaning of AlN and GaN surfaces. Journal of Applied Physics, 1998, 84, 5248-5260.	1.1	277
2	Dielectric Barrier, Etch Stop, and Metal Capping Materials for State of the Art and beyond Metal Interconnects. ECS Journal of Solid State Science and Technology, 2015, 4, N3029-N3047.	0.9	118
3	Plasma enhanced atomic layer deposition of SiN <i>x</i> :H and SiO2. Journal of Vacuum Science and Technology A: Vacuum, Surfaces and Films, 2011, 29, .	0.9	101
4	Fourier transform infrared spectroscopy investigation of chemical bonding in low-k a-SiC:H thin films. Journal of Non-Crystalline Solids, 2011, 357, 2970-2983.	1.5	92
5	Thermal conductivity and thermal boundary resistance of atomic layer deposited high- <i>k</i> dielectric aluminum oxide, hafnium oxide, and titanium oxide thin films on silicon. APL Materials, 2018, 6, .	2.2	82
6	Review—Investigation and Review of the Thermal, Mechanical, Electrical, Optical, and Structural Properties of Atomic Layer Deposited High- <i>k</i> Dielectrics: Beryllium Oxide, Aluminum Oxide, Hafnium Oxide, and Aluminum Nitride. ECS Journal of Solid State Science and Technology, 2017, 6, N189-N208.	0.9	81
7	Dependence of (0001) GaN/AlN valence band discontinuity on growth temperature and surface reconstruction. Journal of Applied Physics, 1998, 84, 2086-2090.	1.1	77
8	Influence of network bond percolation on the thermal, mechanical, electrical and optical properties of high and low-k a-SiC:H thin films. Journal of Non-Crystalline Solids, 2013, 379, 67-79.	1.5	76
9	Investigation of the impact of insulator material on the performance of dissimilar electrode metal-insulator-metal diodes. Journal of Applied Physics, 2014, 116, .	1.1	69
10	Intrinsic stress effect on fracture toughness of plasma enhanced chemical vapor deposited SiNx:H films. Thin Solid Films, 2010, 518, 4898-4907.	0.8	59
11	Research Updates: The three M's (materials, metrology, and modeling) together pave the path to future nanoelectronic technologies. APL Materials, 2013, 1, .	2.2	58
12	Film Property Requirements for Hermetic Low-k a-SiO _x C _y N _z :H Dielectric Barriers. ECS Journal of Solid State Science and Technology, 2012, 1, N115-N122.	0.9	56
13	Interfacial Defect Vibrations Enhance Thermal Transport in Amorphous Multilayers with Ultrahigh Thermal Boundary Conductance. Advanced Materials, 2018, 30, e1804097.	11.1	55
14	Wet Chemical Processing of (0001)Si 6Hâ€ s iC Hydrophobic and Hydrophilic Surfaces. Journal of the Electrochemical Society, 1999, 146, 1910-1917.	1.3	54
15	Nanoscale mapping of contact stiffness and damping by contact resonance atomic force microscopy. Nanotechnology, 2012, 23, 215703.	1.3	49
16	Mass and bond density measurements for PECVD a-SiCx:H thin films using Fourier transform-infrared spectroscopy. Journal of Non-Crystalline Solids, 2011, 357, 3602-3615.	1.5	48
17	Intrinsic stress fracture energy measurements for PECVD thin films in the SiOxCyNz:H system. Microelectronics Reliability, 2009, 49, 721-726.	0.9	45
18	A method to extract absorption coefficient of thin films from transmission spectra of the films on thick substrates. Journal of Applied Physics, 2012, 111, .	1.1	45

#	Article	IF	CITATIONS
19	Mechanical properties of high porosity low- <i>k</i> dielectric nano-films determined by Brillouin light scattering. Journal Physics D: Applied Physics, 2013, 46, 045308.	1.3	45
20	X-ray photoelectron spectroscopy measurement of the Schottky barrier at the SiC(N)/Cu interface. Journal of Vacuum Science and Technology B:Nanotechnology and Microelectronics, 2011, 29, .	0.6	44
21	Elastic properties of porous low-k dielectric nano-films. Journal of Applied Physics, 2011, 110, .	1.1	40
22	Defect structure and electronic properties of SiOC:H films used for back end of line dielectrics. Journal of Applied Physics, 2014, 115, 234508.	1.1	40
23	Measurement of the band gap by reflection electron energy loss spectroscopy. Journal of Electron Spectroscopy and Related Phenomena, 2016, 212, 74-80.	0.8	40
24	Gas source molecular beam epitaxy of scandium nitride on silicon carbide and gallium nitride surfaces. Journal of Vacuum Science and Technology A: Vacuum, Surfaces and Films, 2014, 32, .	0.9	38
25	Impact of VUV photons on SiO2 and organosilicate low-k dielectrics: General behavior, practical applications, and atomic models. Applied Physics Reviews, 2019, 6, .	5.5	38
26	X-ray photoelectron spectroscopy analysis of GaN/(0001)AlN and AlN/(0001)GaN growth mechanisms. Journal of Applied Physics, 1999, 86, 5584-5593.	1.1	36
27	Valence band discontinuity, surface reconstruction, and chemistry of (0001), (0001̄), and (11̄00) 2H–AlN/6H–SiC interfaces. Journal of Applied Physics, 1999, 86, 4483-4490.	1.1	34
28	The influence of hydrogen on the chemical, mechanical, optical/electronic, and electrical transport properties of amorphous hydrogenated boron carbide. Journal of Applied Physics, 2015, 118, .	1.1	34
29	Elastic modulus of low- <i>k</i> dielectric thin films measured by load-dependent contact-resonance atomic force microscopy. Journal of Materials Research, 2009, 24, 2960-2964.	1.2	33
30	X-ray photoelectron spectroscopy investigation of the Schottky barrier at low-k a-SiO(C):H/Cu interfaces. Applied Physics Letters, 2011, 99, .	1.5	32
31	Fracture properties of hydrogenated amorphous silicon carbide thin films. Acta Materialia, 2012, 60, 682-691.	3.8	31
32	Detection of surface electronic defect states in low and high- <i>k</i> dielectrics using reflection electron energy loss spectroscopy. Journal of Materials Research, 2013, 28, 2771-2784.	1.2	29
33	Full Characterization of the Mechanical Properties of 11–50 nm Ultrathin Films: Influence of Network Connectivity on the Poisson's Ratio. Nano Letters, 2017, 17, 2178-2183.	4.5	29
34	Thermodynamic Stability of Lowâ€ <i>k</i> Amorphous SiOCH Dielectric Films. Journal of the American Ceramic Society, 2016, 99, 2752-2759.	1.9	28
35	Hydrogen desorption kinetics and band bending for 6H–SiC(0 0 0 1) surfaces. Surface Science, 2009, 603, 3104-3118.	0.8	27
36	Ultraviolet radiation effects on paramagnetic defects in low-κ dielectrics for ultralarge scale integrated circuit interconnects. Applied Physics Letters, 2010, 97, .	1.5	27

#	Article	IF	CITATIONS
37	Defect-induced bandgap narrowing in low-k dielectrics. Applied Physics Letters, 2015, 107, 082903.	1.5	27
38	Microstructure-mechanical properties correlation in irradiated amorphous SiOC. Scripta Materialia, 2018, 146, 316-320.	2.6	27
39	Remote H2/N2 plasma processes for simultaneous preparation of low-k interlayer dielectric and interconnect copper surfaces. Journal of Vacuum Science and Technology B:Nanotechnology and Microelectronics, 2012, 30, 031212.	0.6	26
40	Spin transport, magnetoresistance, and electrically detected magnetic resonance in amorphous hydrogenated silicon nitride. Applied Physics Letters, 2016, 109, .	1.5	26
41	X-ray photoelectron diffraction from (3×3) and (â^š3×â^š3)R 30° (0001)Si 6H–SiC surfaces. Journal of Applied Physics, 1998, 84, 6042-6048.	1.1	25
42	Valence band discontinuity of the (0001) 2H-GaN / (111) 3C-SiC interface. Journal of Electronic Materials, 1999, 28, L34-L37.	1.0	25
43	Simple bond energy approach for non-destructive measurements of the fracture toughness of brittle materials. Thin Solid Films, 2007, 515, 7232-7241.	0.8	25
44	Defects and electronic transport in hydrogenated amorphous SiC films of interest for low dielectric constant back end of the line dielectric systems. Journal of Applied Physics, 2013, 114, .	1.1	23
45	Tuning the properties of a complex disordered material: Full factorial investigation of PECVD-grown amorphous hydrogenated boron carbide. Materials Chemistry and Physics, 2016, 173, 268-284.	2.0	23
46	Nanoscale Chemical-Mechanical Characterization of Nanoelectronic Low- <i>k</i> Dielectric/Cu Interconnects. ECS Journal of Solid State Science and Technology, 2016, 5, P3018-P3024.	0.9	23
47	Thermal conductivity and sound velocity measurements of plasma enhanced chemical vapor deposited a-SiC:H thin films. Thin Solid Films, 2011, 519, 7895-7898.	0.8	22
48	X-ray Photoelectron Spectroscopy Investigation of the Schottky Barrier at a-BN:Hâ^•Cu Interfaces. Electrochemical and Solid-State Letters, 2011, 14, H478.	2.2	22
49	Validation of a correction procedure for removing the optical effects from transmission spectra of thin films on substrates. Journal of Applied Physics, 2012, 112, .	1.1	22
50	Investigation of the Dielectric and Mechanical Properties for Magnetron Sputtered BCN Thin Films. ECS Journal of Solid State Science and Technology, 2015, 4, N3122-N3126.	0.9	22
51	Atomic force microscopy for nanoscale mechanical property characterization. Journal of Vacuum Science and Technology B:Nanotechnology and Microelectronics, 2020, 38, .	0.6	22
52	Defect chemistry and electronic transport in low- \hat{I}^{ϱ} dielectrics studied with electrically detected magnetic resonance. Journal of Applied Physics, 2016, 119, .	1.1	21
53	Ex Situ and in Situ Methods for Oxide and Carbon Removal from AlN and GaN Surfaces. Materials Research Society Symposia Proceedings, 1995, 395, 739.	0.1	20
54	Chemical Vapor Cleaning of 6Hâ€ S iC Surfaces. Journal of the Electrochemical Society, 1999, 146, 3448-3454.	1.3	20

#	Article	IF	CITATIONS
55	Rigidity Percolation in Plasma Enhanced Chemical Vapor Deposited a-SiC:H Thin Films. ECS Transactions, 2010, 33, 185-194.	0.3	19
56	Conquering the Lowâ€ <i>k</i> Death Curve: Insulating Boron Carbide Dielectrics with Superior Mechanical Properties. Advanced Electronic Materials, 2016, 2, 1600073.	2.6	19
57	XPS Measurement of the SiC/AlN Band-Offset at the (0001) Interface. Materials Research Society Symposia Proceedings, 1995, 395, 375.	0.1	18
58	Tunable Plasticity in Amorphous Silicon Carbide Films. ACS Applied Materials & Interfaces, 2013, 5, 7950-7955.	4.0	18
59	Tailored amorphous silicon carbide barrier dielectrics by nitrogen and oxygen doping. Thin Solid Films, 2013, 531, 552-558.	0.8	18
60	Valence and conduction band offsets at amorphous hexagonal boron nitride interfaces with silicon network dielectrics. Applied Physics Letters, 2014, 104, .	1.5	18
61	Influence of hydrogen content and network connectivity on the coefficient of thermal expansion and thermal stability for a-SiC:H thin films. Journal of Non-Crystalline Solids, 2014, 389, 78-85.	1.5	18
62	Band diagram for low-k/Cu interconnects: The starting point for understanding back-end-of-line (BEOL) electrical reliability. Microelectronics Reliability, 2016, 63, 201-213.	0.9	18
63	Valence band offset at the amorphous hydrogenated boron nitride-silicon (100) interface. Applied Physics Letters, 2012, 101, 042903.	1.5	17
64	Toughening Thinâ€Film Structures with Ceramic‣ike Amorphous Silicon Carbide Films. Small, 2014, 10, 253-257.	5.2	17
65	Investigation of atomic layer deposited beryllium oxide material properties for high-k dielectric applications. Journal of Vacuum Science and Technology B:Nanotechnology and Microelectronics, 2014, 32, .	0.6	17
66	Atomic layer deposited lithium aluminum oxide: (In)dependency of film properties from pulsing sequence. Journal of Vacuum Science and Technology A: Vacuum, Surfaces and Films, 2015, 33, .	0.9	17
67	Mechanical properties of low- and high- <i>k</i> dielectric thin films: A surface Brillouin light scattering study. Journal of Applied Physics, 2016, 119, .	1.1	17
68	Review—Beyond the Highs and Lows: A Perspective on the Future of Dielectrics Research for Nanoelectronic Devices. ECS Journal of Solid State Science and Technology, 2019, 8, N159-N185.	0.9	17
69	Nanoscale Buckling of Ultrathin Low- <i>k</i> Dielectric Lines during Hard-Mask Patterning. Nano Letters, 2015, 15, 3845-3850.	4.5	16
70	Breaking network connectivity leads to ultralow thermal conductivities in fully dense amorphous solids. Applied Physics Letters, 2016, 109, .	1.5	16
71	Nanoscale tomographic reconstruction of the subsurface mechanical properties of low- <i>k</i> high-aspect ratio patterns. Nanotechnology, 2016, 27, 485706.	1.3	16

72 Dry Ex Situ Cleaning Processes for  ( 0001 ) Si 6H‣iC Surfaces. Journal of the Electrochemical Society, 1999, 146, 2648-2651. 15

#	Article	IF	CITATIONS
73	Valence and conduction band alignment at ScN interfaces with 3C-SiC (111) and 2H-GaN (0001). Applied Physics Letters, 2014, 105, 081606.	1.5	14
74	Role of CMOS Back-End Metals as Active Electrodes for Resistive Switching in ReRAM Cells. ECS Journal of Solid State Science and Technology, 2017, 6, N1-N9.	0.9	14
75	Kinetics of Ga and In desorption from (7×7) Si(111) and (3×3) 6H-SiC(0001) surfaces. Surface Science, 2008, 602, 405-415.	0.8	13
76	Valence band offset and Schottky barrier at amorphous boron and boron carbide interfaces with silicon and copper. Applied Surface Science, 2013, 285, 545-551.	3.1	13
77	Noncontact optical metrologies for Young's modulus measurements of nanoporous low-k dielectric thin films. Journal of Nanophotonics, 2013, 7, 073094.	0.4	13
78	Bandgap measurements of low-k porous organosilicate dielectrics using vacuum ultraviolet irradiation. Applied Physics Letters, 2014, 104, .	1.5	13
79	Band Alignment at Molybdenum Disulphide/Boron Nitride/Aluminum Oxide Interfaces. Journal of Electronic Materials, 2016, 45, 983-988.	1.0	13
80	Demonstration of a reliable high-performance and yielding Air gap interconnect process. , 2010, , .		12
81	Thermal Conductivity Measurement of Low-k Dielectric Films: Effect of Porosity and Density. Journal of Electronic Materials, 2014, 43, 746-754.	1.0	12
82	Mechanical property changes in porous low- <i>k</i> dielectric thin films during processing. Applied Physics Letters, 2014, 105, .	1.5	12
83	Carbonâ€Enriched Amorphous Hydrogenated Boron Carbide Films for Very‣owâ€ <i>k</i> Interlayer Dielectrics. Advanced Electronic Materials, 2017, 3, 1700116.	2.6	12
84	Full characterization of ultrathin 5-nm low- <mml:math xmlns:mml="http://www.w3.org/1998/Math/MathML"><mml:mi>k</mml:mi> dielectric bilayers: Influence of dopants and surfaces on the mechanical properties. Physical Review Materials, 2020, 4, .</mml:math 	0.9	12
85	Valence Band Offset at a-B:H and a-BP:H/Si Interfaces. ECS Journal of Solid State Science and Technology, 2012, 1, P250-P253.	0.9	11
86	Photoemission investigation of the Schottky barrier at the Sc/3C-SiC (111) interface. Physica Status Solidi (B): Basic Research, 2015, 252, 391-396.	0.7	11
87	Combinatorial survey of fluorinated plasma etching in the silicon-oxygen-carbon-nitrogen-hydrogen system. Journal of Vacuum Science and Technology A: Vacuum, Surfaces and Films, 2016, 34, .	0.9	11
88	Network structure of a-SiO:H layers fabricated by plasma-enhanced chemical vapor deposition: Comparison with a-SiC:H layers. Journal of Non-Crystalline Solids, 2016, 440, 49-58.	1.5	11
89	Optimization of amorphous semiconductors and low-/high-k dielectrics through percolation and topological constraint theory. MRS Bulletin, 2017, 42, 39-44.	1.7	11
90	Thermal conductivity of plasma deposited amorphous hydrogenated boron and carbon rich thin films. Journal of Nuclear Materials, 2019, 514, 154-160.	1.3	11

#	Article	IF	CITATIONS
91	Observation of Radiation-Induced Leakage Current Defects in MOS Oxides With Multifrequency Electrically Detected Magnetic Resonance and Near-Zero-Field Magnetoresistance. IEEE Transactions on Nuclear Science, 2020, 67, 228-233.	1.2	11
92	Interface and layer periodicity effects on the thermal conductivity of copper-based nanomultilayers with tungsten, tantalum, and tantalum nitride diffusion barriers. Journal of Applied Physics, 2020, 128, .	1.1	11
93	Thermal Conductivity Enhancement in Ion-Irradiated Hydrogenated Amorphous Carbon Films. Nano Letters, 2021, 21, 3935-3940.	4.5	11
94	Valence and conduction band offsets at low-k a-SiOxCy:H/a-SiCxNy:H interfaces. Journal of Applied Physics, 2014, 116, 113703.	1.1	10
95	Cleaning of pyrolytic hexagonal boron nitride surfaces. Surface and Interface Analysis, 2015, 47, 798-803.	0.8	10
96	Characterization of Porous BEOL Dielectrics for Resistive Switching. ECS Transactions, 2016, 72, 35-50.	0.3	10
97	Back-end-of-line a-SiOxCy:H dielectrics for resistive memory. AIP Advances, 2018, 8, .	0.6	10
98	X-ray photoelectron spectroscopy investigation of the valence band offset at beryllium oxide-diamond interfaces. Diamond and Related Materials, 2020, 101, 107647.	1.8	10
99	Plasma Enhanced Atomic Layer Deposition of SiN:H Using N ₂ and Silane. ECS Transactions, 2010, 33, 365-373.	0.3	9
100	Desorption and sublimation kinetics for fluorinated aluminum nitride surfaces. Journal of Vacuum Science and Technology A: Vacuum, Surfaces and Films, 2014, 32, .	0.9	9
101	Analysis of Low-k Dielectric Thin Films on Thick Substrates by Transmission FTIR Spectroscopy. ECS Journal of Solid State Science and Technology, 2015, 4, N3146-N3152.	0.9	9
102	Nanoscale chemical structure variations in nano-patterned and nano-porous low-k dielectrics: A comparative photothermal induced resonance and infrared spectroscopy investigation. Vibrational Spectroscopy, 2016, 86, 223-232.	1.2	9
103	Observation of space charge limited current by Cu ion drift in porous low-k/Cu interconnects. Applied Physics Letters, 2010, 96, 091903.	1.5	8
104	Probing limits of acoustic nanometrology using coherent extreme ultraviolet light. Proceedings of SPIE, 2013, , .	0.8	8
105	Moisture-assisted cracking and atomistic crack path meandering in oxidized hydrogenated amorphous silicon carbide films. Journal of Applied Physics, 2013, 113, .	1.1	8
106	Effects of vacuum-ultraviolet irradiation on copper penetration into low-k dielectrics under bias-temperature stress. Applied Physics Letters, 2015, 106, 012904.	1.5	8
107	Band alignment at AlN/Si (111) and (001) interfaces. Journal of Applied Physics, 2015, 118, .	1.1	8
108	Boron and high-k dielectrics: Possible fourth etch stop colors for multipattern optical lithography processing. Journal of Vacuum Science and Technology A: Vacuum, Surfaces and Films, 2017, 35, 021510.	0.9	8

#	Article	IF	CITATIONS
109	Acoustic Phonons and Mechanical Properties of Ultra-Thin Porous Low-k Films: A Surface Brillouin Scattering Study. Journal of Electronic Materials, 2018, 47, 3942-3950.	1.0	8
110	Hydrogen effects on the thermal conductivity of delocalized vibrational modes in amorphous silicon nitride <mml:math xmlns:mml="http://www.w3.org/1998/Math/MathML"> <mml:mo>(</mml:mo><mml:mi>a</mml:mi><mml:mi< td=""><td>text>âð.9/mm</td><td>nl:mstext><mm< td=""></mm<></td></mml:mi<></mml:math 	text>âð .9 /mm	nl:mstext> <mm< td=""></mm<>
111	5, . Thermal and Chemical Integrity of Ru Electrode in Cu/TaO _x /Ru ReRAM Memory Cell. ECS Journal of Solid State Science and Technology, 2019, 8, N220-N233.	0.9	8
112	Characterization of very low thermal conductivity thin films. Journal of Thermal Analysis and Calorimetry, 2014, 115, 1541-1550.	2.0	7
113	Hydrogen desorption from hydrogen fluoride and remote hydrogen plasma cleaned silicon carbide (0001) surfaces. Journal of Vacuum Science and Technology A: Vacuum, Surfaces and Films, 2015, 33, .	0.9	7
114	Molecular layer deposition using cyclic azasilanes, maleic anhydride, trimethylaluminum, and water. Journal of Vacuum Science and Technology A: Vacuum, Surfaces and Films, 2017, 35, .	0.9	7
115	Relationships between chemical structure, mechanical properties and materials processing in nanopatterned organosilicate fins. Beilstein Journal of Nanotechnology, 2017, 8, 863-871.	1.5	7
116	Electrically detected magnetic resonance and near-zero field magnetoresistance in 28Si/28SiO2. Journal of Applied Physics, 2021, 130, 065701.	1,1	7
117	Thermal stability of Ti, Pt, and Ru interfacial layers between seedless copper and a tantalum diffusion barrier. Journal of Vacuum Science and Technology B:Nanotechnology and Microelectronics, 2013, 31, .	0.6	6
118	Atomic scale trap state characterization by dynamic tunneling force microscopy. Applied Physics Letters, 2014, 105, 052903.	1.5	6
119	Picosecond ultrasonic study of surface acoustic waves on titanium nitride nanostructures. Journal of Applied Physics, 2015, 117, .	1.1	6
120	Hydrogen desorption kinetics for aqueous hydrogen fluoride and remote hydrogen plasma processed silicon (001) surfaces. Journal of Vacuum Science and Technology A: Vacuum, Surfaces and Films, 2015, 33, .	0.9	6
121	Measurement of the vacuum-ultraviolet absorption spectrum of low-k dielectrics using X-ray reflectivity. Applied Physics Letters, 2018, 112, .	1.5	6
122	Thermal conductivity-structure-processing relationships for amorphous nano-porous organo-silicate thin films. Journal of Porous Materials, 2020, 27, 565-586.	1.3	6
123	Probing thermal conductivity of subsurface, amorphous layers in irradiated diamond. Journal of Applied Physics, 2021, 129, .	1.1	6
124	Effects of 29Si and 1H on the near-zero field magnetoresistance response of Si/SiO2 interface states: Implications for oxide tunneling currents. Applied Physics Letters, 2021, 119, .	1.5	6
125	Cu film thermal stability on plasma cleaned polycrystalline Ru. Journal of Vacuum Science and Technology B:Nanotechnology and Microelectronics, 2012, 30, .	0.6	5
126	Study of viscoplastic deformation in porous organosilicate thin films for ultra low-k applications. Applied Physics Letters, 2013, 102, .	1.5	5

#	Article	IF	CITATIONS
127	Complete Elemental Analysis of Low-ka-SiC:H Thin Films by Transmission FTIR Spectroscopy. ECS Journal of Solid State Science and Technology, 2014, 3, N52-N57.	0.9	5
128	Time-dependent dielectric breakdown measurements of porous organosilicate glass using mercury and solid metal probes. Journal of Vacuum Science and Technology A: Vacuum, Surfaces and Films, 2014, 32, .	0.9	5
129	Preface: Materials, metrology, and modeling for a future beyond CMOS technology. APL Materials, 2018, 6, .	2.2	5
130	Narrowing of the Boolchand intermediate phase window for amorphous hydrogenated silicon carbide. Journal of Non-Crystalline Solids, 2018, 499, 252-256.	1.5	5
131	Modeling and simulation of Cu diffusion and drift in porous CMOS backend dielectrics. APL Materials, 2018, 6, 066101.	2.2	5
132	Heat capacities, entropies, and Gibbs free energies of formation of low-k amorphous Si(O)CH dielectric films and implications for stability during processing. Journal of Chemical Thermodynamics, 2019, 128, 320-335.	1.0	5
133	Influence of topological constraints on ion damage resistance of amorphous hydrogenated silicon carbide. Acta Materialia, 2019, 165, 587-602.	3.8	5
134	Advances in metrology for the determination of Young's modulus for low-k dielectric thin films. , 2012, , .		4
135	Measurements of Schottky barrier at the low-k SiOC:H/Cu interface using vacuum ultraviolet photoemission spectroscopy. Applied Physics Letters, 2015, 107, .	1.5	4
136	Thermodynamics of amorphous SiN(O)H dielectric films synthesized by plasmaâ€enhanced chemical vapor deposition. Journal of the American Ceramic Society, 2018, 101, 2017-2027.	1.9	4
137	Underlying role of mechanical rigidity and topological constraints in physical sputtering and reactive ion etching of amorphous materials. Physical Review Materials, 2018, 2, .	0.9	4
138	Reliability and performance limiting defects in low-к dielectrics for use as interlayer dielectrics. , 2010, , .		3
139	Characterization of ultrathin films by laser-induced sub-picosecond photoacoustics with coherent extreme ultraviolet detection. Proceedings of SPIE, 2012, , .	0.8	3
140	Role of Nano-Porosity in Plasma Enhanced Chemical Vapor Deposition of Hermetic low-k a-SiOCN:H Dielectric Barrier Materials. ECS Transactions, 2013, 45, 27-45.	0.3	3
141	Influence of porosity on electrical properties of low-k dielectrics irradiated with vacuum-ultraviolet radiation. Applied Physics Letters, 2016, 109, 122902.	1.5	3
142	Radiation induced leakage currents in dense and porous low-k dielectrics. , 2016, , .		3
143	Resistive Switching Comparison between Cu/TaOx/Ru and Cu/TaOx/Pt Memory Cells. ECS Transactions, 2017, 75, 13-23.	0.3	3
144	Modeling and Simulation of Cu Diffusion in Porous Low-k Dielectrics. ECS Transactions, 2017, 77, 121-132.	0.3	3

#	Article	IF	CITATIONS
145	The Effect of Edge Compliance on the Contact between a Spherical Indenter and a High-Aspect-Ratio Rectangular Fin. Experimental Mechanics, 2018, 58, 1157-1167.	1.1	3
146	Energetics of porous amorphous low-k SiOCH dielectric films. Journal of Chemical Thermodynamics, 2019, 139, 105885.	1.0	3
147	Band offsets at amorphous hydrogenated boron nitride/high- <i>k</i> oxide interfaces from x-ray photoelectron spectroscopy with charging effects analysis. Journal of Vacuum Science and Technology B:Nanotechnology and Microelectronics, 2020, 38, .	0.6	3
148	A Selectively Colorful yet Chilly Perspective on the ^{Highs} and _{Lows} of Dielectric Materials for CMOS Nanoelectronics. , 2020, , .		3
149	Removal of Fluorine From a Si (100) Surface by a Remote RF Hydrogen Plasma. Materials Research Society Symposia Proceedings, 1995, 386, 357.	0.1	2
150	An Electron Paramagnetic Resonance Study of Defects in Interlayer Dielectrics. ECS Transactions, 2011, 35, 747-756.	0.3	2
151	Spectroscopic method for measuring refractive index. Applied Optics, 2013, 52, 4477.	0.9	2
152	Hardness Studies of RF Sputtered Deposited BCN Thin Films. ECS Transactions, 2014, 58, 147-153.	0.3	2
153	Atomic Layer Deposited Hybrid Organic-Inorganic Aluminates as Potential Low-k Dielectric Materials. Materials Research Society Symposia Proceedings, 2015, 1791, 15-20.	0.1	2
154	Modeling and Simulation of Cu Drift in Porous Low-k Dielectrics. ECS Transactions, 2017, 80, 327-337.	0.3	2
155	Valence and conduction band offsets at beryllium oxide interfaces with silicon carbide and III-V nitrides. Journal of Vacuum Science and Technology B:Nanotechnology and Microelectronics, 2019, 37, 041206.	0.6	2
156	Topological Constraint Theory Analysis of Rigidity Transition in Highly Coordinate Amorphous Hydrogenated Boron Carbide. Frontiers in Materials, 2019, 6, .	1.2	2
157	Extrinsic time-dependent dielectric breakdown of low-k organosilicate thin films from vacuum-ultraviolet irradiation. Journal of Vacuum Science and Technology A: Vacuum, Surfaces and Films, 2017, 35, 021509.	0.9	2
158	Extraction of dipolar coupling constants from low-frequency electrically detected magnetic resonance and near-zero field magnetoresistance spectra via least squares fitting to models developed from the stochastic quantum Liouville equation. Journal of Applied Physics, 2021, 130, 234401.	1.1	2
159	Ex Situ and In Situ Methods for Complete Oxygen and Non-Carbidic Carbon Removal from (0001)SI 6H-SiC Surfaces. Materials Research Society Symposia Proceedings, 1996, 423, 563.	0.1	1
160	Impact of Film Stress on Nanoidentation Fracture Toughness Measurements for PECVD SiNx:H Films. ECS Transactions, 2009, 19, 455-466.	0.3	1
161	Defects in low-κ dielectrics and etch stop layers for use as interlayer dielectrics in ULSI. , 2010, , .		1

Mechanical properties of hydrogenated amorphous silicon carbide thin films. , 2010, , .

1

#	Article	IF	CITATIONS
163	Transmission Fourier Transform Infra-red Spectroscopy Investigation of Structure Property Relationships in Low-k SiO _x C _y :H Dielectric Thin Films. Materials Research Society Symposia Proceedings, 2012, 1520, 1.	0.1	1
164	(Invited) Dielectric Damage. ECS Transactions, 2014, 60, 733-738.	0.3	1
165	Decoupling of Ion Diffusivity and Electromobility in Porous Dielectrics. ECS Transactions, 2016, 72, 233-240.	0.3	1
166	Effects of cesium ion-implantation on mechanical and electrical properties of organosilicate low-k films. Applied Physics Letters, 2016, 108, 202901.	1.5	1
167	Effects of cesium ion implantation on the mechanical and electrical properties of porous SiCOH low-k dielectrics. Journal of Vacuum Science and Technology A: Vacuum, Surfaces and Films, 2017, 35, 061506.	0.9	1
168	Identifying Defects Responsible For Leakage Currents in Thin Dielectric Films. , 2018, , .		1
169	High Toughness and Moisture Insensitive Hydrogenated Amorphous Silicon Carbide Films for MEMS/NEMS. ECS Transactions, 2010, 33, 257-261.	0.3	0
170	Electron paramagnetic resonance studies of interlayer dielectrics. , 2011, , .		0
171	Development of Voltammetry-Based Techniques for Characterization of Porous Low-k/Cu Interconnect Integration Reliability. ECS Transactions, 2011, 35, 757-771.	0.3	0
172	Schottky Barrier Height at Dielectric Barrier/Cu Interface in Low-K/Cu Interconnects. ECS Transactions, 2011, 35, 849-860.	0.3	0
173	Valence Band Offset at Amorphous Boron Carbide / Silicon Interfaces. Materials Research Society Symposia Proceedings, 2013, 1576, 1.	0.1	0
174	Reliable characterization of materials and nanostructured systems <<50nm using coherent EUV beams. , 2016, , .		0
175	Impact of Embedment of Cu/TaOx/Ru on Its Device Performance. ECS Transactions, 2017, 80, 911-921.	0.3	0
176	Correction to: The Effect of Edge Compliance on the Contact between a Spherical Indenter and a High-Aspect-Ratio Rectangular Fin. Experimental Mechanics, 0, , .	1.1	0